

# Impact of Different Dielectric Fluids on Surface Roughness During EDM Machining of AISI 4140 Steel

Naveen Porwal, Love Kishore Sharma, Anil Kumar Sharma  
Department of Mechanical Engineering  
Jaipur Institute of Technology  
Jaipur, India

**Abstract:-** Electric Discharge Machining (EDM) is an alternative machining process to traditional machining process for the precise machining of complex shaped electrically conductive machine parts. The main objective of this research work is to study the impact of EDM conditions (Pulse on time, peak current, voltage and types of dielectric) on SR during machining of AISI 4140 steel using RSM based on face centered design. Also an effort is made with optimized EDM conditions to formulate the relationship between machining conditions and responses for desired responses. The SEM analysis has also been carried out to examine the surface morphology of machined surfaces of test specimens. The pulse on time, peak current, voltage, and types of dielectric are found significant EDM conditions that affect the SR. The SR is directly proportional to pulse on time & peak current for both Kerosene and deionized water as dielectric fluid. Also, the prediction ability of the developed model has been found significant.

**Keywords:-** EDM , SEM, Surface Roughness, Dielectric Fluid.

## I. INTRODUCTION

Electric Discharge Machining (EDM) is an alternative machining process to traditional machining process for the precise machining of complex shaped electrically conductive machine parts. Now days, due to global competitiveness, manufacturing industries are more concerned about the quality of their products. During EDM machining, the machining conditions play important role. The quality of machined part depends on the proper selection of the EDM conditions [1]. Therefore, for the desired EDM output, judicious selection of the machining condition requires. Therefore, many researchers have applied different techniques for the optimization of EDM conditions for minimum surface roughness during EDM machining of different materials.

Balasubramanian and Senthilvelan [2] used RSM for the study of the impact of EDM conditions on MRR, SR and TW during the EDM machining of EN8 and D3 steel. The high value of MRR and TWR were obtained during the machining of D3 steel using cast electrode in comparison to sintered electrode. Salcedo et al.[3] Investigated the impact of  $P_{on}$ ,  $D_f$ , type of polarity, type of electrode and  $I_p$  on

MRR, SR and TW during the EDM machining of Inconel 600 using copper-carbon, graphite and copper electrodes. The maximum MRR, maximum SR and maximum TW were achieved with negative polarity. Vaidya and Shinde[4] employed Taguchi methodology to optimize the WEDM conditions for minimum SR and maximum MRR during the machining of 11 hot die steel using brass electrode. The  $P_{on}$  and  $V$  were found main influencing parameters for SR while  $P_{on}$  and  $P_{off}$  were found most significant parameters for MRR.

Kumar and Kumar[5] employed Taguchi methodology to study the impact of EDM conditions on MRR at the time of machining of mild steel using copper tool. The  $I_p$  was found main affecting condition that influence the MRR followed by  $P_{on}$ ,  $P_{off}$  and  $V$ . Dhakad and Vimal [6] utilized principal component analysis to optimize the WEDM conditions For MRR, machining time and gap voltage during the machining of 45A Alloy Steel. Among the all WEDM parameters, the open voltage was identified as main influencing parameter. Brar et al.[7]utilized the Taguchi methodology to optimize the effect of WEDM conditions for minimum SR and maximum MRR during the machining of aluminum 6061 alloy. For MRR and SR,  $P_{on}$  and  $I_p$  were found most significant conditions and MRR increases with increase in  $P_{on}$  and  $I_p$ .

Moghaddam and Kolahan[8] employed Taguchi methodology to examine the impact of EDM parameters on MRR, TW and SR during the EDM machining of AISI2312 steel. The  $I_p$  was most significant parameter that affects the MRR while  $P_{on}$  found most significant parameter for SR and TW. Vikash et al.[9] made a comparison between two sets of the values of MRR to examine the impact of carbon during the EDM machining of EN19 and EN41steels. The current was found most significant EDM parameter that affects MRR for both materials. Shashikant et al.[10] used RSM for the investigation of the impact of EDM parameters on SR during the EDM machining of EN-19 steel. The  $I_p$  was found most significant parameter for SR. Das et al. [11] used artificial bee colony algorithm for the selection of optimum EDM parameters for maximum MRR and minimum SR. The predicted and experimental values of responses were found are in good agreement to each other. It was also found that SR and MRR increase with increase in  $P_{on}$ , and  $I_p$ .

From the review of literature, it is clear that number of research was done to optimize the EDM conditions for desired responses. Some researchers made efforts to examine the impact of EDM conditions on the various responses. Very less effort was made to investigate and compare the effect of different type of dielectric fluids on different responses. The AISI 4140 steel is a chromium-manganese-molybdenum grade is used for making the dies for plastic injection moulds, extrusion dies for thermoplastics and for compression moulds. Therefore, this study is focus on the study of the impact of EDM basic parameters with two types of dielectric fluids (Kerosene and deionized water) SR during the machining AISI 4140 steel.

#### ➤ Experimentation and Measurement

In this study, peak current, open gap voltage, pulse on time and type of dielectric (kerosene and de-ionized water) were selected as EDM conditions. The range of EDM machining conditions i.e maximum and minimum values of peak current, open gap voltage, pulse on time and types of dielectric fluids were selected by considering several factors like type of material, type of electrode, range given in the published literature and according to machine specification. The table 1 represents the selected range and levels of EDM machining conditions according to face centered design based on response surface methodology. The copper electrode of diameter 10 mm was used for EDM machining of work piece. The electrode is kept at negative polarity during the machining while work-piece is kept at positive polarity. For the all experiments CNC based EDM machine “Smart ZNC” manufactured by Electronica India limited was used.

EDM conditions	Type	Levels		
		Minimum	Maximum	Mean
Voltage (V)	Numeric	10	40	25
Peak current (A)	Numeric	10	30	20
Pulse on ( $\mu$ s)	Numeric	50	150	100
Dielectric fluids	Categorical	Kerosene	De-ionized water	

Table 1:- EDM Conditions and Levels

The table 2 represents the design matrix for experimentation in actual form of EDM conditions. The design matrix contained total 40 numbers of experiments i.e 20 with kerosene and 20 with de-ionized water.

The performance of mechanical parts is based on the SR since mechanical properties like tensile strength; impact strength fatigue etc. depends on the surface roughness of the machined parts. The SR is calculated

upon the various parameters but most commonly used parameter is surface roughness values. In the present study, center line average (Ra) of the work pieces after the EDM machining was measured making use of a portable surface tester and the readings were recorded with three times repeated measurements. The measured values of center line average (CLA) surface roughness of machined specimens along with design matrix are presented in the table 2.

St d	Ru n	A:Voltage (V)	B: Peak current (A)	C:Pulse on time ( $\mu$ s)	D: Dielectric	MRR (mg/min)	Surface roughness (Microns)
1	34	10	10	50	Kerosene	108.9	2.538
2	29	40	10	50	Kerosene	77.8	1.243
3	13	10	30	50	Kerosene	159.4	4.385
4	7	40	30	50	Kerosene	122.2	2.813
5	8	10	10	150	Kerosene	180.7	5.795
6	15	40	10	150	Kerosene	161.6	3.661
7	26	10	30	150	Kerosene	234.6	7.328
8	16	40	30	150	Kerosene	202.3	5.033
9	33	10	20	100	Kerosene	152.4	4.61
10	17	40	20	100	Kerosene	124.3	3.18
11	32	25	10	100	Kerosene	123.6	3.114
12	36	25	30	100	Kerosene	172.8	4.893
13	4	25	20	50	Kerosene	112.9	2.662
14	18	25	20	150	Kerosene	192.4	5.489
15	23	25	20	100	Kerosene	138.4	4.103
16	19	25	20	100	Kerosene	134.8	4.08
17	2	25	20	100	Kerosene	143.3	4.292
18	1	25	20	100	Kerosene	136.5	4.441
19	39	25	20	100	Kerosene	139.7	4.137
20	6	25	20	100	Kerosene	136.3	4.188
21	14	10	10	50	De-ionized	109.1	1.82
22	35	40	10	50	De-ionized	85.0	1.103
23	31	10	30	50	De-ionized	171.7	3.988
24	27	40	30	50	De-ionized	134.4	3.072
25	22	10	10	150	De-ionized	159.9	6.351
26	10	40	10	150	De-ionized	140.8	4.693
27	38	10	30	150	De-ionized	218.9	8.5264
28	21	40	30	150	De-ionized	186.6	6.531
29	37	10	20	100	De-ionized	147.9	5.006
30	25	40	20	100	De-ionized	119.7	3.448
31	9	25	10	100	De-ionized	117.2	3.217
32	40	25	30	100	De-ionized	171.3	5.808
33	28	25	20	50	De-ionized	123.0	2.634
34	24	25	20	150	De-ionized	174.5	6.33
35	11	25	20	100	De-ionized	139.4	4.198
36	5	25	20	100	De-ionized	136.8	4.3
37	3	25	20	100	De-ionized	133.9	4.033
38	20	25	20	100	De-ionized	143.3	4.313
39	30	25	20	100	De-ionized	138.6	4.21
40	12	25	20	100	De-ionized	141.8	4.4

Table 2:- Design matrix in actual form and measurement results

➤ *Development of Empirical Prediction Models for Surface Roughness*

To achieve the one objective of the current research work *i.e* development of prediction models for surface roughness, the experimental results along with design matrix have been input into the design expert software 8.0.4.1.

➤ *Validation of the Assumptions of ANOVA for Surface Roughness*

The first step for the development of empirical models is the diagnosis of the assumptions of analysis of variance (ANOVA). The ANOVA is based on the two assumptions *i.e* assumption of “normal distribution of population” and assumption of “homogeneity of variance”. To inspect the viability of assumptions for residual of SR, the Box-Cox plot of the residuals of SR is shown in Fig.1. The Box-Cox transformation is employed to improve the normality of residuals or make the data normally distributed which was not normally distributed. It is a group of transformations that make the data normalize which were not normally distributed by identify a suitable value of Lambda. The Lambda value shows the power on the response to which all data should be raised. The Box and Cox transformation increase the normality and homogeneity of the data[12].

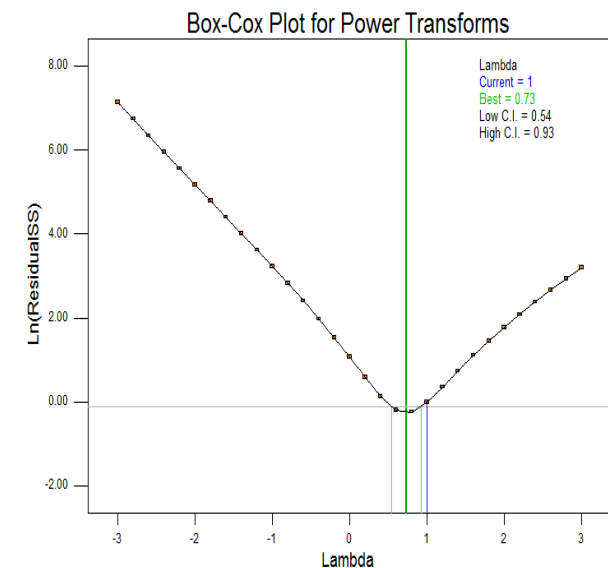


Fig 1:- Box-Cox plot for surface roughness

The figure 1 represents the Box-Cox plots for the residuals of SR. In the plot, the blue line represents the current value of lambda while the best value of lambda is represented by green line. In the figure, the present value of Lambda is “1” while the best value of lambda is 0.73. Therefore, according to Box-Cox transformation the power transformation on the surface roughness is required to increase the normality, linearity and homogeneity of the residuals for surface roughness. Now, after the Box-Cox transformation, the first step is to diagnosis the assumptions of ANOVA.

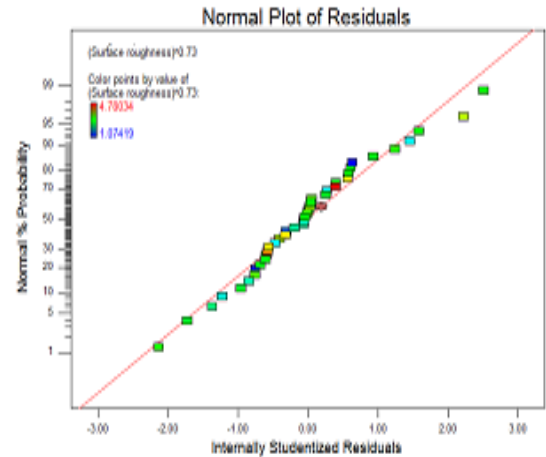


Fig 2:- Normal probability plot for residuals of surface roughness

To validate the first assumption of ANOVA *i.e* assumption of normal distribution of population (residuals), the normal probability plot for residuals of surface roughness are represents in figure 2.

The graph between the residuals and percentage of normal probability is indicated by normal probability plot. The normal probability plot shows whether the residuals follow the assumption of normal distribution or not. If distribution of residuals is normal, the normal percentage probability of residuals will resemble on a straight line in the plot. The figures 2 represent that mostly residuals for surface roughness falls on straight line. That indicates that residuals for surface roughness are normally distributed.

To the validation of second assumption of ANOVA *i.e* assumption of homogeneity of variance, residuals versus the predicted response is required. The figure 3 represents the plot for surface roughness for residuals versus the predicted response respectively. For the validation of the second assumption of ANOVA, the plots should not follow any certain pattern. The figures represents that there is no specific pattern follow by the figures. Therefore residuals of surface roughness follow the second assumption of ANOVA.

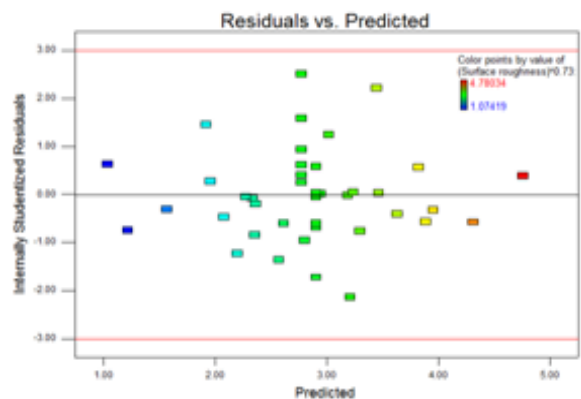


Fig 3:- Plot between residuals and predicted surface roughness

In the current research work, the analysis of variance was carried out at the confidence level of 95%. The reduce ANOVA table for SR after the Box-Cox transformation followed by forward/backward elimination method is represents in table 3.

Source	Sum of squares	Degree of freedom	Mean square	F-Value	p-value	Prob> F
Model	22.548	9	2.505	382.522		0.0001
A-Voltage (V)	2.985	1	2.985	455.714		0.0001
B-Peak current (A)	4.601	1	4.601	702.551		0.0001
C-Pulse on (µs)	14.060	1	14.060	2146.800		0.0001
D-Dielectric	0.175	1	0.175	26.720		0.0001
AC	0.075	1	0.075	11.484		0.0020
AD	0.056	1	0.056	8.616		0.0063
BC	0.090	1	0.090	13.707		0.0009
BD	0.079	1	0.079	12.071		0.0016
CD	0.426	1	0.426	65.034		0.0001
Residual	0.196	30	0.007			
Lack of Fit	0.154	20	0.008	1.808		0.1682
Pure Error	0.043	10	0.004			
Cor Total	22.744	39				
Std. Dev.	0.081		R-Squared			0.991
Mean	2.837		Adj R-Squared			0.989
C.V. %	2.852		Pred R-Squared			0.987
PRESS	0.302		Adeq Precision			91.938

Table 3:- Reduce ANOVA table for SR after Box - Cox Transformation

Table 3 indicates that “Prob. > F” for surface roughness prediction model is less than 0.05, so, model is significant. Also,, the “Prob. > F” for V, I<sub>p</sub>, P<sub>on</sub>, dielectric, interaction terms of V and P<sub>on</sub>, V and dielectric, I<sub>p</sub> and P<sub>on</sub>, I<sub>p</sub> and dielectric, P<sub>on</sub> and dielectric are less than 0.05, that shows the SR prediction model along these all terms are significant i.e these all terms have effect on SR. The “Prob. > F” for lack-of-fit is 0.1682 which is higher than 0.05, so it is insignificant, which is required to model fitting. The R<sup>2</sup> value and adjusted R<sup>2</sup> value are 0.991 and 0.989 respectively, which is very close to each other. Adequate precision is equal to 91.938 which indicate adequate model discrimination.

*Prediction models*

The surface roughness prediction models prediction models are given as:

With kerosene  
 $(SR)^{0.73} = 0.757 - 0.0202 * Voltage + 0.057 * Peakcurrent + 0.02 * Pulseontime - 0.00009 * Voltage * Pulseontime - 0.00015 * Peakcurrent * Pulseontime$  (1)

With de-ionized water  
 $(SR)^{0.73} = -0.123 - 0.013 * Voltage + 0.07 * Peakcurrent + 0.025 * Pulseontime - 0.00009 * Voltage * Pulseontime - 0.00015 * Peakcurrent * Pulseontime$  (2)

**II. INFLUENCE OF EDM CONDITIONS ON SURFACE ROUGHNESS**

The figure 4 and 5 indicates the variation of SR with respect to voltage during the EDM machining using kerosene and de-ionized as dielectric respectively. From the figures, it was revealed that SR continuously decreases with increase in voltage from 10 to 40 volts. During EDM, metal is removed from the surface of work piece due to melting and evaporation. Due to the melting and evaporation, craters on the surface of work piece formed. The size of craters depends on the energy per spark per unit time[1]. The discharge time increases with increase in voltage. The higher discharge time will lead to wider average discharge gap. This will decrease the number of discharge cycles within a given period. Hence, it will decrease the discharge energy per unit time. Further with decrease in discharge energy, the size of craters also decreases which decrease the surface roughness of machined parts [13].

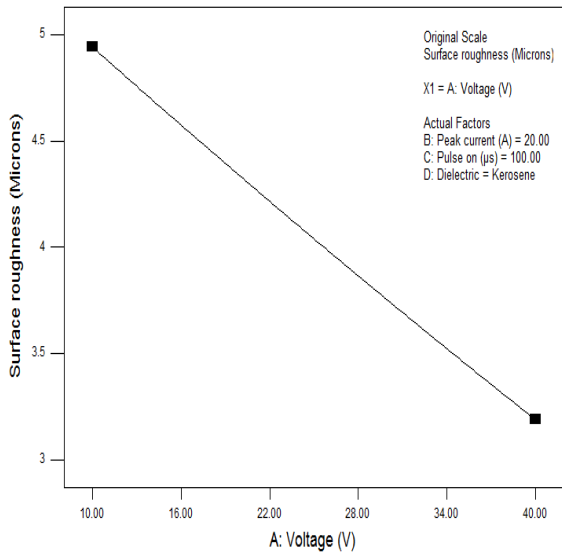


Fig 4:- Impact of voltage on surface roughness with kerosene

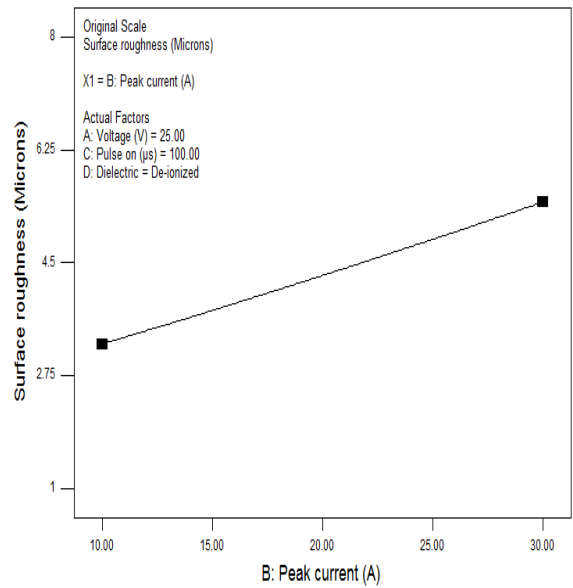


Fig 7:- Impact of I<sub>p</sub> on SR with de-ionized water

The figure 6 and 7 indicates the variation of surface roughness with respect to I<sub>p</sub> during EDM machining with kerosene and de-ionized water as dielectric fluid respectively. From the plots it was revealed that SR continuously increases with increase in peak current from 10A to 30 A. At the high peak current, intensely discharge generated which strike the surfaces of the work piece, which further creates the larger size craters on the surface of work piece. Hence deteriorates the surface of work piece[14].

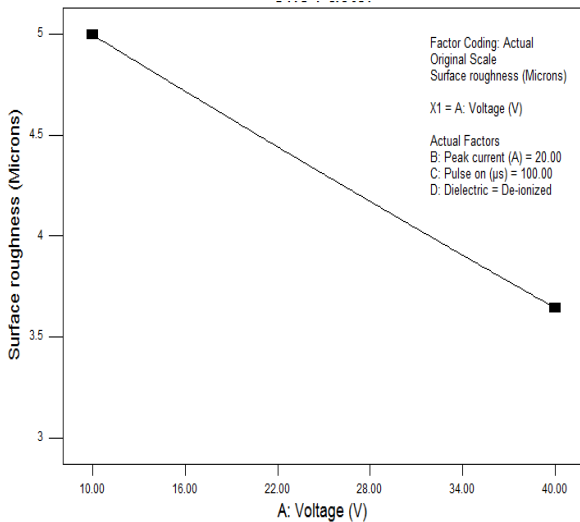


Fig 5:- Impact of voltage on surface roughness with deionized water

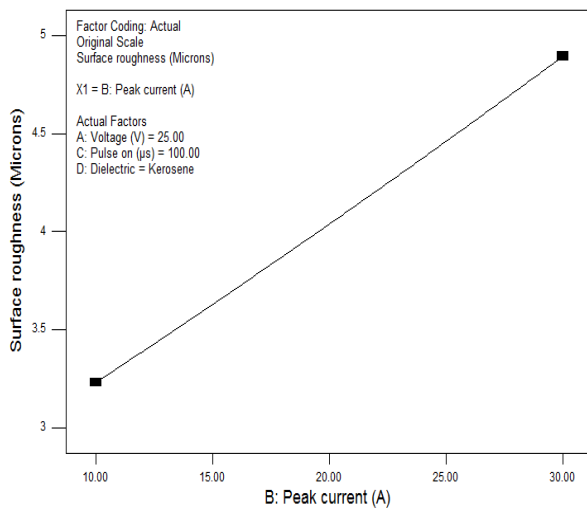


Fig 6:- Impact of peak current on surface roughness with kerosene

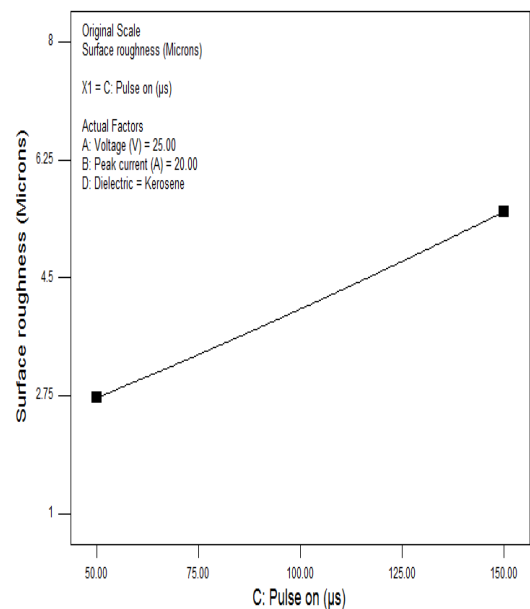


Fig 8:- Impact of P<sub>on</sub> on SR with kerosene

The effect of pulse on time on surface roughness was shown in figures 8 and 9 during the EDM machining with kerosene and de-ionized water as dielectric fluid respectively. From the both figures it was revealed that surface roughness continuously increases with increase in pulse on time from 50 microseconds to 150 microseconds.

The amount of discharge energy depends on the  $P_{on}$ . The amount of discharge energy at the interface of work piece and tool increases with increase in  $P_{on}$ , this further expands the channel of plasma between the work piece and tool. Due to the expanded plasma channel, large size of craters formed at the surface of work piece. This further increases the surface roughness of machined surface[15].

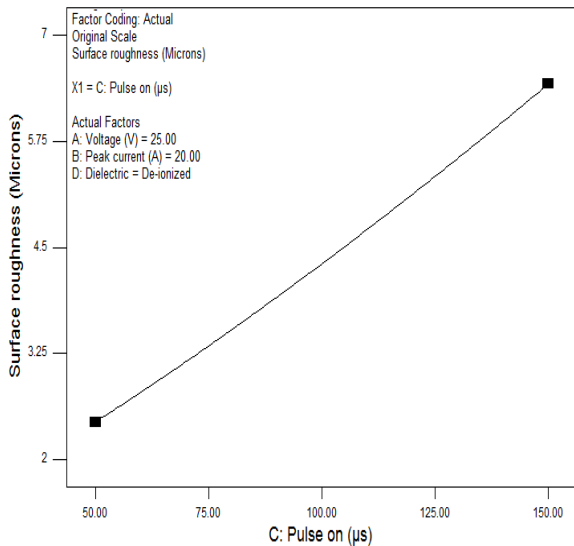


Fig 9:- Impact of  $P_{on}$  on SR with deionized water

The figure 10 shows the impact of both dielectric fluids at the mean values of voltage, peak current and pulse on time on surface roughness. The value of SR achieved is higher with de-ionized water as compared to kerosene. It is because of the way that the cooling rate of molten material is higher with de-ionized water than the kerosene. Therefore heat is quickly dissipated from the melted specimen surface to with dielectric water. Due to this, adhesion and re-solidification of the molten material takes place on the machined surface, which results in poor surface finish[16].

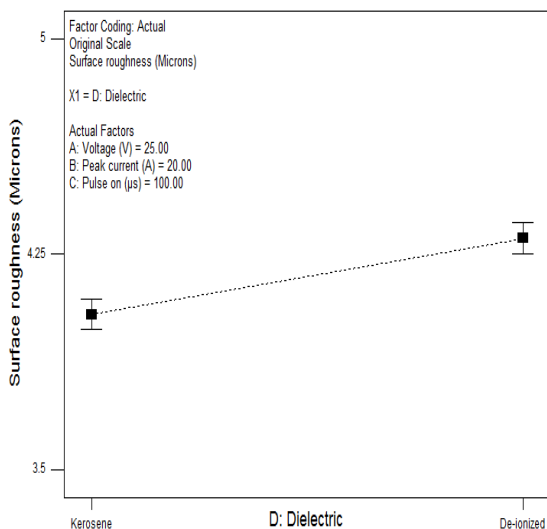


Fig 10:- Impact of types of dielectric on SR

### III. SURFACE MORPHOLOGY ANALYSIS

Surface morphology study of machined surfaces are carried out using scanning electron microscopy (SEM) in order to analyze the effect of EDM conditions on responses such as MRR and SR. The figure 11 and 12 shows the scanning electron microscopy of the surfaces that obtained during EDM machining at 40 V voltage, 50 microseconds pulse rate, 10 A peak current with kerosene and de-ionized water respectively while the figure 13 and 14 shows the scanning electron microscopy of the surfaces that obtained during EDM machining at 10 V voltage, 150 microseconds pulse rate, 30 A peak current with kerosene and de-ionized water respectively. From the figure 11 and 12 it was shown that for the lower value of peak current, lower value of pulse on time and higher value of voltage, surface finish achieved with de-ionized water is better than the kerosene. Less surface damage due to deep craters of varying sizes was found with kerosene as compare to de-ionized water. That indicates the low surface roughness at 40 V voltage, 50 microseconds pulse rate, 10 A peak current with de-ionized water as compared to kerosene. However, small cracks were observed with de-ionized water. From the figure 13 and 14 it was observed that machined surface that were obtained at high value of pulse on time, high value of peak current, low value of voltage shows very rough surface with both dielectric fluids. The surface obtained with de-ionized water exhibited more roughness as compare to the surface that was obtained with kerosene. This is due to the globules of the debris, melted drops and craters of varying in sizes and cracks. At high pulse on time, high current, high temperature gradient generated due to the thermal energy in the work piece. Due to this erosion takes place from the surface and the debris particles remain attached to the work piece surface. Also, the molten material cooling rate is more rapid with de-ionized water than the kerosene. Therefore heat is quickly transferred from the melted work piece surface to dielectric water quickly. Due to this adhesion and re- solidification of the molten material takes place on the machined surface, which results in poor surface finish.

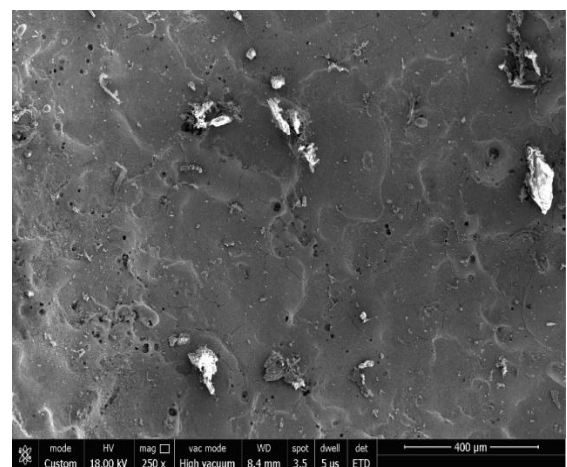


Fig 11:- SEM image at 40V, 10A, 50 microseconds with Kerosene

#### IV. CONCLUSION

This study is focus on the examination of the impact of EDM basic parameters with two types of dielectric fluids on metal removal rate and surface roughness during the machining AISI 4140 steel. Also, an attempt was made to develop surface roughness and metal removal rate prediction models in terms of EDM parameters with different types of dielectric using RSM.

The following major conclusions have been derived:

- The pulse on time, peak current, voltage, and types of dielectric are found significant EDM conditions that affect the SR.
- The interaction of voltage and Pon, voltage and dielectric, Ip and Pon, Ip and dielectric, Pon and dielectric are found significant EDM conditions that affect the SR.
- The R- square value for SR is found as 0.991. This indicates that the developed model has excellent prediction ability.
- The linear variation for surface roughness was obtained with peak current, voltage and pulse on time.
- The surface roughness continuously increases with increase in Pon and increase in Ip and decrease in voltage for both dielectric fluids.
- The minimum SR is achieved at high level of voltage (40 V), low level of Ip (10 A), low level of Pon (50 microseconds) and with kerosene as dielectric fluid.

#### REFERENCES

- [1]. S. S. Habib, "Study of the parameters in electrical discharge machining through response surface methodology approach," *Appl. Math. Model.*, vol. 33, no. 12, pp. 4397–4407, 2009.
- [2]. P. Balasubramanian and T. Senthilvelan, "Optimization of Machining Parameters in EDM Process Using Cast and Sintered Copper Electrodes," *Procedia Mater. Sci.*, vol. 6, no. Icmpec, pp. 1292–1302, 2014.
- [3]. A.T. Salcedo, I. P. Arbizu, and C. J. Luis, "Analytical Modelling of Energy Density and Optimization of the EDM Machining Parameters of Inconel 600," *Metals (Basel)*, vol. 7, no. 5, p. 166, 2017.
- [4]. V. R. Vaidya and B. R. Shinde, "Process Parameter Optimization of Wire EDM for H11 material using RSM and Desirability Function Approach," no. 7, pp. 542–546, 2017.
- [5]. V. Kumar and P. Kumar, "Improving Material Removal Rate and Optimizing Various machining Parameters in EDM," *Int. J. Eng. Sci.*, vol. 06, no. 06, pp. 64–68, 2017.
- [6]. A. K. Dhakad and J. Vimal, "Multi responses optimization of wire EDM process parameters using Taguchi approach coupled with principal component analysis methodology," vol. 9, no. 2, pp. 61–74, 2017.
- [7]. G. S. Brar, S. Singh, and H. Garg, "Optimization of Wire EDM Parameters for Fabrication of Micro Channels," vol. 9, no. 10, pp. 1729–1732, 2015.

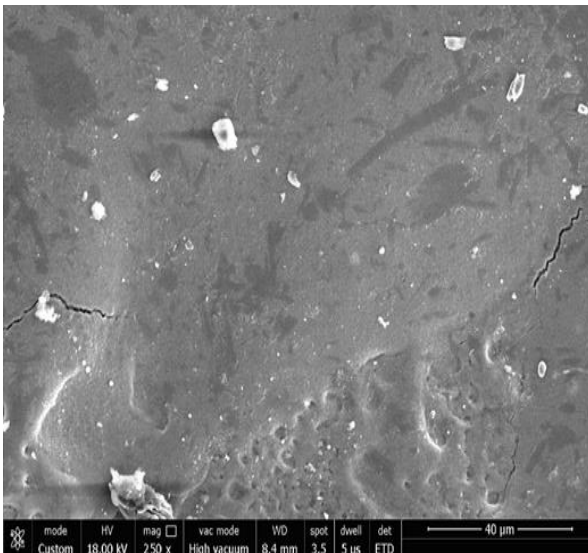


Fig 12:- SEM image at 40V, 10A, 50 microseconds with Dielectric water

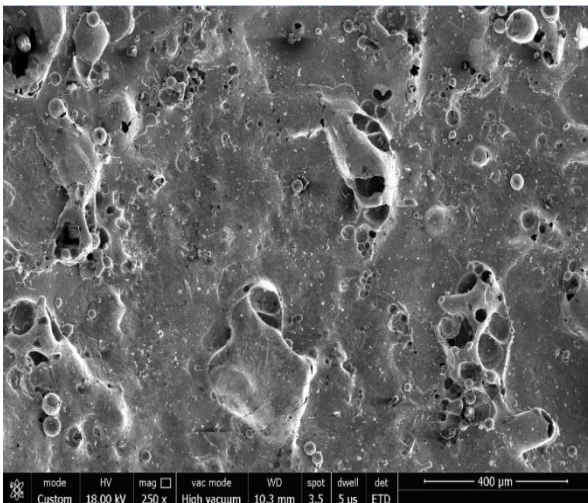


Fig 13:- SEM image at 10V, 30A, 150 microseconds with Kerosene

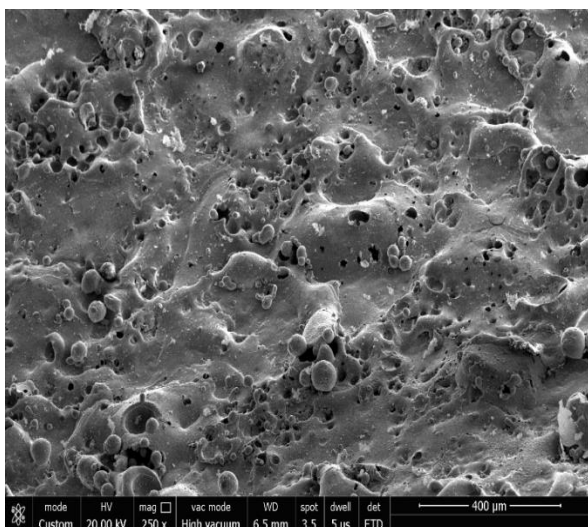


Fig 14:- SEM image at 10V, 30A, 150 microseconds with de-ionized water

- [8]. Moghaddam, M.A and Kolahan, F. (2014). Modeling and optimization of surface roughness of AISI2312 hot worked steel in EDM based on mathematical modeling and genetic algorithm, *International Journal of Engineering*, 23(3), 417-424.
- [9]. Vikas, Shashikant, A. K. Roy, and K. Kumar, "Effect and Optimization of Machine Process Parameters on MRR for EN19 & EN41 Materials Using Taguchi," *Procedia Technol.*, vol. 14, pp. 204–210, 2014.
- [10]. Shashikant, A. K. Roy, and K. Kumar, "Effect and Optimization of Various Machine Process Parameters on the Surface Roughness in EDM for an EN19 Material Using Response Surface Methodology," *Procedia Mater. Sci.*, vol. 5, pp. 1702–1709, 2014.
- [11]. M. K. Das, K. Kumar, T. K. Barman, and P. Sahoo, "Investigation on electrochemical machining of EN31 steel for optimization of MRR and surface roughness using artificial bee colony algorithm," *Procedia Eng.*, vol. 97, pp. 1587–1596, 2014.
- [12]. B. Bhardwaj, R. Kumar, and P. K. Singh, "Effect of machining parameters on surface roughness in end milling of AISI 1019 steel," *Proc. Inst. Mech. Eng. Part B J. Eng. Manuf.*, vol. 228, no. 5, pp. 704–714, 2014.
- [13]. P. N. Singh, , K. Raghukandan, , M. Rathinasabapathi, and B.C. Pai,. "Electric discharge machining of Al-10%SiCP as-cast metal matrix composite". *Journal of Materials Processing Technology*, Vol. 155–156, pp.1653–1657,2004.
- [14]. M. A. R. Khan, M.M.Rahman, K.Kadrigama, M. a. Maleque, and M.Ishak, "Prediction of surface roughness of Ti-6Al-4V in electrical discharge machining: A regression model," *J. Mech. Eng. Sci.*, vol. 1, no. December, pp. 16–24, 2011.
- [15]. S. Daneshmand, V. Monfared, and A. A. Lotfi Neyestanak, "Effect of Tool Rotational and Al<sub>2</sub>O<sub>3</sub> Powder in Electro Discharge Machining Characteristics of NiTi-60 Shape Memory Alloy," *Silicon*, pp. 1–11, 2016.
- [16]. G. Kibria, B. R. Sarkar, B. B. Pradhan, and B. Bhattacharyya, "Comparative study of different dielectrics for micro-EDM performance during microhole machining of Ti-6Al-4V alloy," *Int. J. Adv. Manuf. Technol.*, vol. 48, no. 5–8, pp. 557–570, 2010.